ELSEVIER

Journal of Alloys and Compounds 434–435 (2007) 203–206

Journal of ALLOYS AND COMPOUNDS

www.elsevier.com/locate/jallcom

Studies on the crystallization kinetics of Cu-reinforced partially crystalline $Cu_{47}Ti_{33}Zr_{11}Ni_8Si_1$ metallic glass composite

S. Venkataraman [a,*], J. Eckert [a,b], L. Schultz [b], D.J. Sordelet [c]

[a] FG Physikalische Metallkunde, FB 11 Material-und Geowissenschaften, Technische Universität Darmstadt,
Petersenstraße 23, D-64287 Darmstadt, Germany
[b] IFW Dresden, Postfach 27 00 16, D-01171 Dresden, Germany
[c] Materials and Engineering Physics Program, US Department of Energy, Ames Laboratory, 107 Metals Development, Ames, IA 50011, USA

Abstract

The crystallization kinetics of partially crystalline $Cu_{47}Ti_{33}Zr_{11}Ni_8Si_1$ gas atomized powder (GAP) and composites was studied by differential scanning calorimetry. The activation energy for crystallization as determined by the Kissinger equation is nearly equal for the particle-free powder (3.13 ± 0.40 eV) and the composite (3.11 ± 0.22 eV). The activation energy of crystallization derived from isothermal annealing experiments is nearly similar for the GAP (4.53 ± 0.40 eV) and the composite (4.25 ± 0.40 eV). The values of the Avrami exponent suggest that the crystallization is diffusion controlled. The local Avrami exponent suggests that surface nucleation is active in GAP but bulk crystallization dominates in milled composite powder.

Keywords: Metallic glasses; Powder metallurgy; Phase transition; Kinetics; Thermal analysis

1. Introduction

Preparation of bulk metallic glassy matrix composites has yielded improvements in tensile and compressive strains to failure [1]. Bulk metallic glass composites produced by consolidation of glassy powders have many advantages: unlimited dimension, no restrictions on reinforcement size and volume fraction non very limited interfacial reactions and the possibility to produce parts of complex shape [2]. $Cu_{47}Ti_{33}Zr_{11}Ni_8Si_1$ is one of the best bulk glass-forming alloys in the Cu–Ti–Ni–Zr system [3]. Crystallization kinetics of fully glassy $Cu_{47}Ti_{33}Zr_{11}Ni_8Si_1$ gas atomized powder reinforced with Cu particulates was studied earlier [4]. Addition of Cu particles does not have affect thermal stability and nucleation and growth in the glassy matrix. However, not much is known about the kinetics of crystallization of partially crystallized amorphous alloys/composites. It is interesting to analyze the influence of crystallites present in as-quenched glassy powders on the consolidation/shaping of powders for potential use.

In this contribution, the kinetics of crystallization of partially crystalline glassy $Cu_{47}Ti_{33}Zr_{11}Ni_8Si_1$ reinforced with 25 vol.% Cu particles as prepared by ball milling has been investigated by differential scanning calorimetry. Local Avarami exponent was used to explain details of the nucleation and growth behavior upon devitrification.

2. Experimental

High-pressure gas atomization was used to synthesize the $Cu_{47}Ti_{33}Zr_{11}Ni_8Si_1$ powders [5]. Blending of gas-atomized powder (GAP) with 25 vol.% Cu was done in a Retsch 4000 planetary mill [4]. Structural characterization of the GAP as well as the composite powder was done by X-ray diffraction (XRD) using a Philips PW1050 diffractometer (Co Kα radiation). The microstructure of the powders were examined using a field emission gun scanning electron microscope (LEO GEMINI 1531) equipped with an in situ-energy dispersive X-ray spectrometer (EDXS). The crystallization kinetics were analyzed by continuous heating (at heating rates ranging from 10 to 80 K/min) as well as by isothermal annealing in a differential scanning calorimeter (Perkin-Elmer DSC-7) under flowing high purity Ar. For isothermal analysis, the samples were first heated to a fixed temperature (at a heating rate of 40 K/min) and held until complete of crystallization. For each individual sample, two successive DSC runs were recorded with the second run serving as a baseline.

3. Results and discussion

Fig. 1 shows continuous heating DSC at a heating rate of 40 K/min for GAP and composite powder. Both DSC traces exhibit a distinct endothermic event characteristic of a glass

---

[*] Corresponding author. Present address: IFW Dresden, Helmholtzstrasse 20, D-01069 Dresden, Germany. Tel.: +49 351 4659644; fax: +49 351 4659452.
E-mail address: s.venkataraman@ifw-dresden.de (S. Venkataraman).

0925-8388/$ – see front matter © 2006 Elsevier B.V. All rights reserved.
doi:10.1016/j.jallcom.2006.08.140

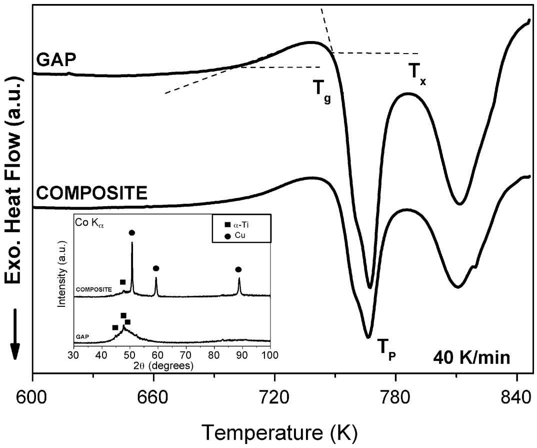

Fig. 1. Constant heating rate DSC scans for $Cu_{47}Ti_{33}Zr_{11}Ni_8Si_1$ GAP and composite powder (*inset*: X-ray diffraction patterns).

transition, T_g, an extended super cooled liquid region and an exothermic event characterizing the onset of crystallization, T_x. The DSC scan for the GAP reveals that the T_g is at 698 K and the T_x occurs at 752 K. The width of the supercooled liquid region is found to be 54 K. The value is smaller than that reported for $Cu_{47}Ti_{34}Zr_{11}Ni_8Si_1$ metallic glass (66 K) produced by copper mold casting [3]. The XRD patterns of the GAP (as-prepared state) and the composite powder after 20 h of ball milling are shown as inset in Fig. 1. In case of GAP, the pattern displays a near amorphous pattern with superimposed crystalline reflections of α-Ti having a lattice constant $a = 0.28963$ nm, $c = 0.46472$ nm, c/a ratio = 1.60. The presence of Ti is also confirmed by SEM as shown in Fig. 2(a), where Ti-rich dendritic crystallites with a size of less than 5 μm are observed in a glassy matrix. EDXS analysis indicates that the dendritic phase is rich in Ti and lean in Cu whereas the amorphous matrix is Cu-rich and Ti-lean. The decrease of the extent of supercooled liquid region can be explained on the basis of the change in the composition of the glassy matrix caused due to the presence of crystalline dendrites. The XRD pattern of the composite powder shows the presence of crystalline Cu peaks superimposed on the broad diffuse scattering maxima from the amorphous phase. The thermal stability data for the composite powder is the same as that for the GAP, suggesting that addition of Cu particles has no distinct effect on the crystallization behavior of the matrix.

Upon continuous heating using different heating rates (not shown here), T_p, defined as the peak temperature of the first exothermic event is shifted to higher temperatures with increasing heating rates. The activation energy for crystallization E_c can be evaluated by means of the Kissinger equation [6].

$$\ln\left(\frac{\phi}{{T_p}^2}\right) = \frac{-E}{RT_p} + \text{constant} \tag{1}$$

where Φ is the heating rate and R the gas constant and T_p stands for the crystallization peak temperature. Fig. 3(a) shows the Kissinger plot. The activation energy calculated from the Kissinger relationship is 3.13 ± 0.40 eV for the GAP and 3.11 ± 0.22 eV for the composite powder. These values are slightly lower than the corresponding values obtained for fully glassy $Cu_{47}Ti_{33}Zr_{11}Ni_8Si_1$ powder and composites with the same volume fraction of Cu particles but with a glassy matrix as has been reported earlier [4] and smaller than 3.69 eV obtained for $Cu_{47}Ti_{33}Zr_{11}Ni_8Si_1$ metallic glass produced by copper mold casting [3].

Isothermal DSC investigations show that all DSC traces (not shown here) exhibit a single exothermic peak after passing a certain incubation period, which decreases with increasing temperature. The kinetics of phase transition are usually analyzed in terms of the generalized theory of phase transition [7]:

$$x_c(t, T) = 1 - \exp(-k(t - \tau)^n) \tag{2}$$

where k is a reaction rate constant, τ the incubation time, and n is the Avrami exponent. Eq. (2) can be rewritten as the Johnson-Mehl-Avrami (JMA) Equation [8].

$$\ln\left[\ln\left(\frac{1}{1-x}\right)\right] = n\ \ln k + n\ \ln(t - \tau) \tag{3}$$

Fig. 4(a) shows the plots of $\ln[\ln(1/1 - x)]$ and $n \ln(t - \tau)$. The Avrami exponent n and the reaction rate constant k can be calculated from the slopes and intercepts of the lines. The values of n range from 2.4 to 3 for the GAP and from 2.9 to 3.1 for the composite powder. The values of the Avrami exponent suggest that the nucleation occurs at a constant rate and is diffusion-controlled [9]. Fig. 2(b) shows the morphology of the crystallization product in the glassy powder, annealed at 723 K for 100 min. Spherical crystals, non-uniform in size (40–150 nm) are uniformly distributed throughout the volume.

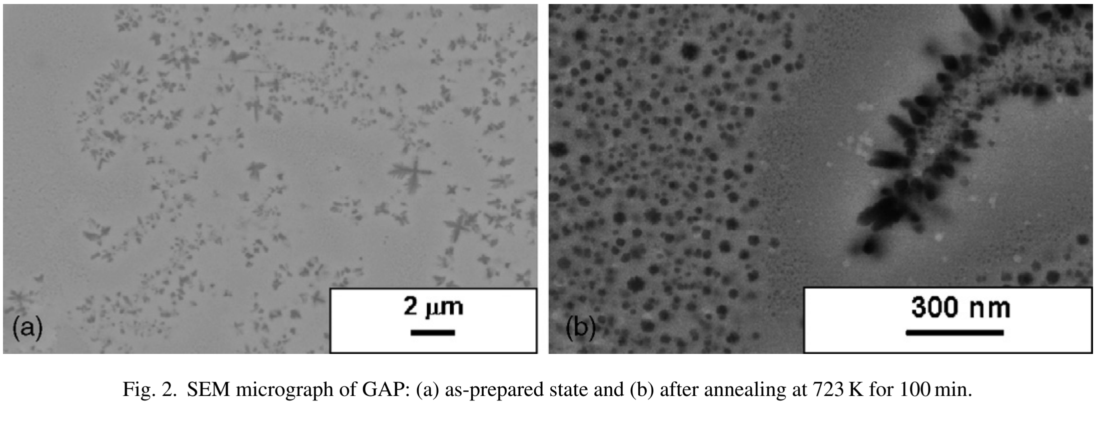

Fig. 2. SEM micrograph of GAP: (a) as-prepared state and (b) after annealing at 723 K for 100 min.

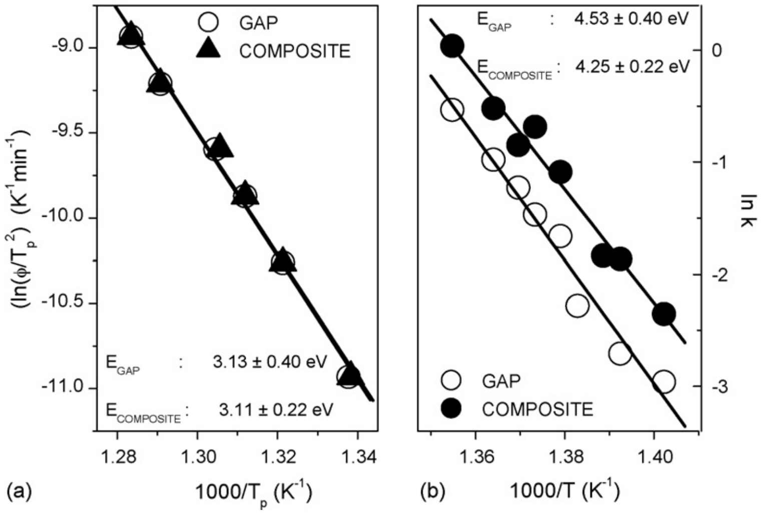

Fig. 3. (a) Kissinger plots and (b) ln *K* vs. 1/*T* plots for $Cu_{47}Ti_{33}Zr_{11}Ni_8Si_1$ GAP and composite powder.

This suggests homogenous nucleation. The local Avrami kinetics exponent, n_{loc} has been often used to highlight changes in the reaction kinetics during the progress of transformation and was calculated [10]:

$$n_{\mathrm{loc}} = \frac{\partial \ln[-\ln(1-x)]}{\partial \ln(t-\tau)} \tag{4}$$

The local value of the Avrami exponent of GAP isothermally annealed at 733 K (Fig. 4(b)) is close to 2, which indicates surface crystallization. With increasing crystallized volume fraction the n_{loc} steadily increases and reaches 3, attributed to bulk crystallization with a constant nucleation rate. In the later stages of crystallization, Avrami exponent decreases suggesting a reduced nucleation rate. This can be attributed to nucleation saturation and three-dimensional growth of crystalline nuclei leading to subsequent crystal impingement [11]. The observed increase in n_{loc} in the last stage of crystallization may be due to errors derived from isothermal DSC. In case of the composite powder, two distinct features are clearly noticed. There is no surface crystallization stage visible and bulk crystallization dominates over the whole range of transformation. Avrami exponent remains constant around 3. Hence, bulk crystallization kinetics of the amorphous alloy is accelerated after mechanical deformation induced by ball milling. Before the onset of bulk crystallization the surface layers of the composite powder begin to crystallize upon mechanical deformation caused by milling. This leads to a reduced volume fraction for surface crystallization in the DSC. Similar observations have been made in ball milled $Fe_{40}Ni_{40}P_{14}B_6$ metallic glass ribbons [12].

The reaction rate constant *k* can be written as [8]:

$$k = k_0 \left[\frac{-E_{\mathrm{c}}}{RT}\right] \tag{5}$$

where k_0 is a constant and E_{c} is the apparent activation energy for crystallization. Fig. 3(b) shows the plot of ln *k* versus 1/*T*. The activation energy for crystallization is 4.53 ± 0.40 and 4.25 ± 0.22 eV for the particle-free and the particle-containing powders, respectively, close to the activation energy

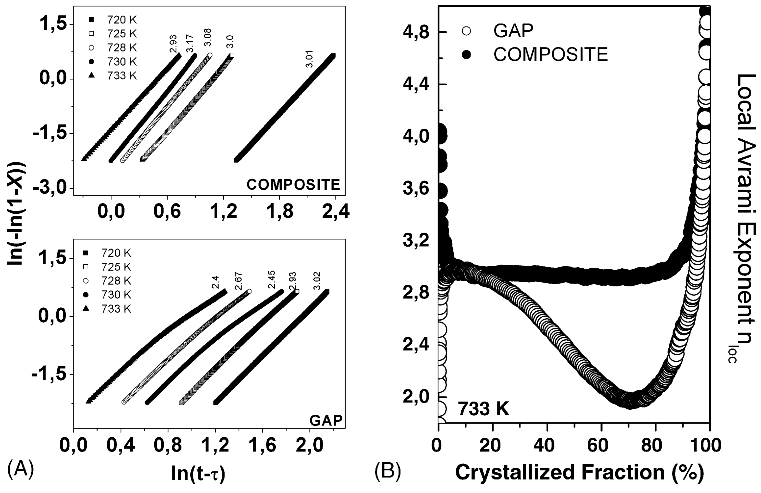

Fig. 4. (a) JMA plots and (b) variation of the local Avrami exponent with crystallized volume fraction for GAP and composite powder.

of $Cu_{47}Ti_{34}Zr_{11}Ni_8$ metallic glass produced by copper mold casting (4.28 ± 0.11 eV) [13]. However, the isothermal activation energy is larger than that calculated for fully amorphous $Cu_{47}Ti_{33}Zr_{11}Ni_8Si_1$ gas atomized powder-based composites [5]. Though there is an order of magnitude difference between the activation energies it is not surprising. In case of the $Zr_{69.5}Cu_{12}Ni_{11}Al_{7.5}$ quasicrystal-forming alloy it has been shown that the activation energy calculated from Arrehnius type relation is 345 kJ/mol and exceeds the value calculated by Kissinger‘s approach (256 kJ/mol) [14]. However, a common behavior of the variation of the activation energy is obtained. Similar findings were reported for amorphous Ni–P [15].

4. Conclusions

The thermal stability and crystallization kinetics of Cu-reinforced partially crystalline $Cu_{47}Ti_{33}Zr_{11}Ni_8Si_1$ glassy matrix composite powders has been studied. The activation energy for crystallization is nearly equal for particle-free and composite powders. Presence of Cu particles and dendritic Ti crystals do not change the crystallization kinetics.

Acknowledgements

The authors thank B. Bartusch, K. Berger and H. Schulze for technical assistance and K. Biswas and S. Deledda for stimulating discussions. Funding by the German Research Foundation under grant no. Ec111/10-1,2 is gratefully acknowledged.

References

[1] C.C. Hays, C.P. Kim, W.L. Johnson, Phys. Rev. Lett. 84 (2000) 2901–2904.
[2] Y. Kawamura, H. Mano, A. Inoue, Scripta Mater. 44 (2000) 1119–1124.
[3] H.C. Yim, R. Busch, W.L. Johnson, J. Appl. Phys. 83 (1998) 7993–7997.
[4] S. Venkataraman, E. Rozhkova, J. Eckert, L. Schultz, D.J. Sordelet, Intermetallics 13 (2005) 833–840.
[5] D.J. Sordelet, E. Rozhkova, P. Huang, P.B. Wheelock, M.F. Besser, M.J. Kramer, M. Calvo-Dahlborg, U. Dahlborg, J. Mater. Res. 17 (2002) 186–198.
[6] H.E. Kissinger, Anal. Chem. 29 (1957) 1702–1706.
[7] M.J. Avrami, J. Chem. Phys. 9 (1941) 177–184.
[8] J.W. Christian, The Theory of Transformation in Metals and Alloys, first ed., Pergamon Press, London, 1975.
[9] R.D. Doherty, in: R.W. Cahn, P. Haasen (Eds.), Physical Metallurgy, North Holland, Amsterdam, 1996, pp. 1364–1505.
[10] A. Calka, A.P. Radlinski, Mater. Sci. Eng. 97 (1988) 241–246.
[11] A. Calka, A.P. Radlinski, J. Mater. Res. 3 (1988) 59–66.
[12] G.J. Fan, M.X. Quan, Z.Q. Hu, W. Löser, J. Eckert, J. Mater. Res. 14 (1999) 3765–3774.
[13] S.C. Glade, J.F. Löffler, S. Bossuyt, W.L. Johnson, M.K. Miller, J. Appl. Phys. 89 (2001) 1573–1579.
[14] U. Köster, J. Meinhardt, S. Roos, R. Busch, Mater. Sci. Eng. A 226–228 (1997) 995–998.
[15] R. Lück, K. Lu, W. Frantz, Scr. Metall. Mater. 28 (1993) 1071–1075.